

Article

# Modeling of Linear and Non-linear Compression Processes of Sunflower Bulk Oilseeds

Abraham Kabutey<sup>1,\*</sup>, David Herak<sup>1</sup>, Himsar Ambarita<sup>2</sup> and Riswanti Sigalingging<sup>3</sup>

<sup>1</sup> Department of Mechanical Engineering, Faculty of Engineering, Czech University of Life Sciences Prague, Kamýcká 129, 165 21, Prague 6 Suchbát, Czech Republic

<sup>2</sup> Department of Mechanical Engineering, Faculty of Engineering, Universitas Sumatera Utara, Jl. Almamater Kampus USU, Medan 20155, Indonesia

<sup>3</sup> Department of Agricultural Engineering, Faculty of Agriculture, Universitas Sumatera Utara, Kampus USU, Prof. A. Sofyan No. 3, Medan 20155, Indonesia

\* Correspondence: kabutey@tf.czu.cz; Tel.: +420-22438-3180

Received: 8 July 2019; Accepted: 31 July 2019; Published: 3 August 2019



**Abstract:** The present study aimed at describing the experimental and theoretical force-deformation curves of sunflower bulk oilseeds at varying initial pressing heights and vessel diameters as well as determining the theoretical pressure and energy along the screw press FL 200 pressing chambers. The design of efficient oil expression systems for industry and small-scale application remains a major challenge to engineers and researchers. In attempting to solve the problem, it is important to understand the linear compression process and to transfer the knowledge to the industry involving mechanical screw presses. The universal compression testing machine at a preset load of 200 kN and a speed of 5 mm·min<sup>-1</sup>, tangent curve model and the screw press FL 200 geometry parameters were applied. The obtained results of pressure and energy along the screw pressing chambers (1–7) ranged from 0.31 to 101.653 MPa and 12.616 to 1231.228 J. Applying the tangent model at  $n = 1$  and  $n = 2$ , the cumulative pressure decreased with increasing vessel diameters while energy increased. The study provides useful information for the analysis of other bulk oilseeds and optimizing the processing parameters of screw press FL 200 and the design and development of new oil presses.

**Keywords:** sunflower bulk oilseeds; compression processes; tangent curve model; screw geometry

## 1. Introduction

There is the concern with the environmental preservation, which is structured both in efforts to optimize energy efficiency and investments in research, development and application of renewable resources, and cleaner technologies [1–4]. Vegetable oil from oilseeds such as sunflower seeds, rapeseeds among others is one of the renewable sources worldwide for application in internal combustion engines [5,6]. However, the design of efficient oil expression systems for industry and small-scale or rural-based operations has been the main challenge to engineers and scientists [7,8].

Mechanical pressing (using a screw or hydraulic presses) and solvent extraction with n-hexane are commonly used commercial oil extraction methods [9–13]. Although the mechanical pressing gives a lower yield compared to the solvent extraction method, it has several advantages including the lower cost of equipment and higher oil quality [14–17]. In the literature, the oil yield using the mechanical pressing process is dependent on particle size, moisture content, heating temperature, heating time, applied pressure and pressing time [18–21]. The press and screw configurations are also factors affecting mechanical oil expression [22]. Generally, mechanical expression of oil requires the application of pressure on the operating conditions, pretreatment and raw material. In addition, for a given pressure, deformation and compression of particles begin to release the oil from the capillaries of particles.

The pressing or compression process can be understood as the process of capillary filtration where the volume of the separated liquid passing through the capillaries is dependent on the applied pressure, diameter of the capillary channel, dynamic viscosity, length of capillary channel and time of applied pressure. The compression process can also be influenced positively if the pressure, diameter and time increase while the dynamic viscosity and length also decrease. The oil expression efficiency, on the other hand, is influenced by the porosity of the cake, yield stress of the solid phase, the compressive force and viscosity of the expressed oil. The general theoretical description of oil expression has been based on the theories of consolidation originally developed for soil mechanics [22,23]. Several studies have been reported on the modeling of oilseed expression resulting in the development of empirical models, Terzaghi-type models and models based on the cell structure of the oilseeds [23–28].

Despite the significant efforts in the modeling development, press design and automation, optimizing the oil expression processing parameters along the screw chambers or lamella positions remain a problem due to the complexity of the mechanisms involved in the continuous dynamic process of the mechanical pressing of oilseeds [29]. In order to design and develop new efficient systems, it is important to understand the linear compression process of oilseeds and the transformation of the results to the non-linear compression process involving mechanical screw presses. This scope of research is limited in the literature. Therefore, the aim of this study was to describe the experimental and theoretical force-deformation curves of sunflower bulk oilseeds, determine the experimental and theoretical deformation energy as well as to determine the theoretical pressure (screw pressure) and energy (screw energy) along the screw pressing chambers of screw press FL 200.

## 2. Materials and Methods

The sunflower bulk oilseeds sample (bulk sample) was used for the linear compression test experiment. Before the experiment, impurities including leaves and pieces of stalks were removed from the bulk sample which has been kept under laboratory conditions. The moisture content of the bulk sample was determined to be 10.14 (% w.b.) using the standard procedure [30] and the relation given by [31] as described in Equation (1) as follows:

$$MC = \left( \frac{m_a - m_b}{m_a} \cdot 100 \right) \quad (1)$$

where  $MC$  is the moisture content in wet basis (% w.b.),  $m_a$  and  $m_b$  are the weights of the bulk sample before and after oven drying at a temperature of 105 °C and a drying time of 17 hours. The universal compression-testing machine (Tempos, Model ZDM 50, Czech Republic) was used to describe the relationship between the compressive force and deformation curve patterns of the bulk sample initial pressing heights at a maximum force of 200 kN and a speed of 5 mm·min<sup>-1</sup> (Figure 1). The initial bulk sample heights at 40, 60 and 80 mm were measured and compressed in each pressing vessel of diameter 60, 80 and 100 mm. The compression test was repeated twice. The deformation values were obtained directly from the compression test. The oil yield and experimental deformation energy [32–34] were calculated using Equation (2) and Equation (3) as follows:

$$OY = \left( \frac{O_w}{O_m} \cdot 100 \right) \quad (2)$$

where  $OY$  is the oil yield (%),  $O_w$  is the weight of oil (g) and  $O_m$  is the initial weight of the bulk sample (g).

$$U = \sum_{n=0}^{n=i-1} \left[ \left( \frac{F_{n+1} + F_n}{2} \right) \cdot (x_{n+1} - x_n) \right] \quad (3)$$

where  $U$  is the experimental deformation energy (J),  $F_{n+1} + F_n$  and  $x_{n+1} - x_n$  are the compressive force (kN) and deformation (mm),  $n$  is the number of data points and  $i$  is the number of sections in which the axis deformation was divided (step measurement was 0.01).

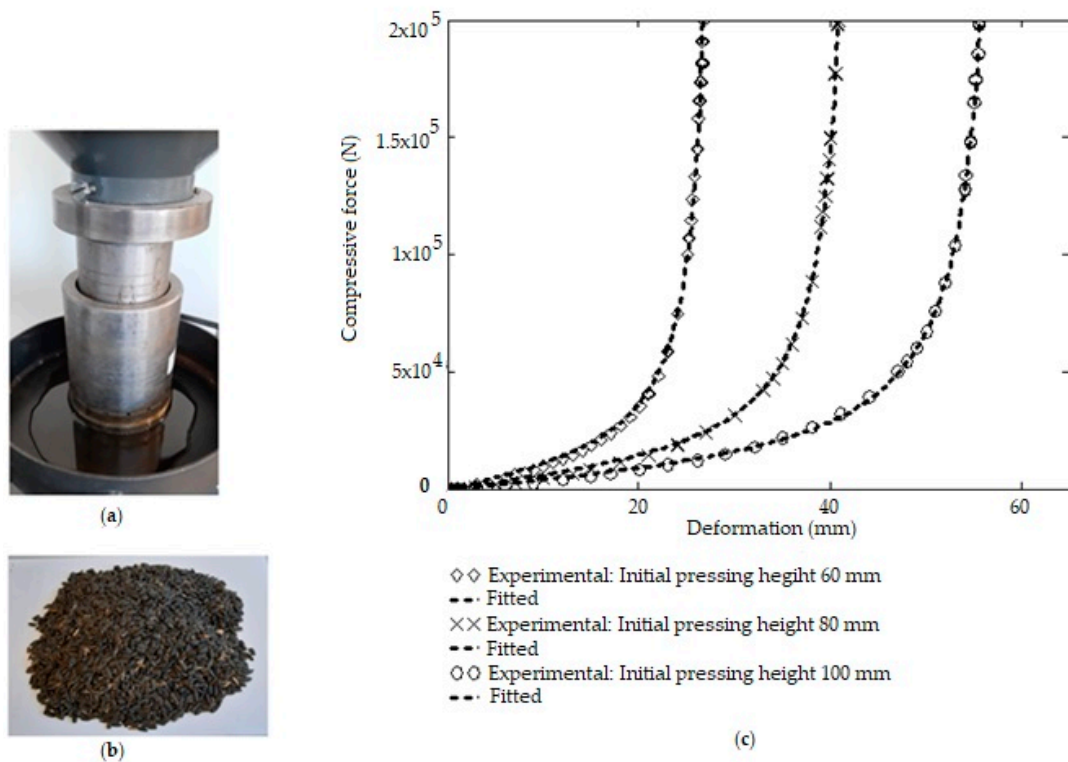


**Figure 1.** (a) Compression test set-up using a vessel diameter of 100 mm with a plunger (similar to vessel diameters of 60 and 80 mm) and a pan for collecting the pressed oil; (b) Sunflower bulk oilseeds; (c) Experimental and fitted dependency between compressive force and deformation curves of sunflower bulk oilseeds at initial heights of 40, 60 and 80 mm (Equation (5)).

The theoretical deformation energy from the compression test was calculated based on the tangent curve mathematical model [35–38], as described in Equations (4)–(6) as follows:

$$F(x) = A \cdot (\tan(B \cdot x))^n \quad (4)$$

$$\int F(x)^{n=1} dx \rightarrow -\frac{A \cdot \ln(\cos(B \cdot x))}{B} \quad (5)$$

$$\int F(x)^{n=2} dx \rightarrow \frac{A \cdot (\tan(B \cdot x) - B \cdot x)}{B} \quad (6)$$

where  $F$  is the force (kN),  $x$  is deformation (mm),  $A$  is the force coefficient of mechanical behavior (kN),  $B$  is the deformation coefficient of mechanical behavior ( $\text{mm}^{-1}$ ),  $n$  is the fitting curve function exponent. Equation (4) describes the theoretical deformation energy of the bulk sample at a specific pressing height where the force is a function of the deformation. Equation (5) and Equation (6) explain the integral of Equation (4) for which  $n = 1$  and  $n = 2$  respectively. For describing the theoretical deformation energy of the bulk sample where the force is a function of different variables such as deformation, pressing height and vessel diameter [32,34], Equation (7) was applied. Equation (8) and Equation (9) explain the integral of Equation (7) for which  $n = 1$  and  $n = 2$ .

$$F(x, H, D) = C \cdot D^2 \cdot \left( \tan\left(G \cdot \frac{x}{H}\right) \right)^n \quad (7)$$

$$T_E^{n=1} : \int F(x, H, D)^{n=1} dx \rightarrow -\frac{C \cdot D^2 \cdot H \cdot \ln\left(\cos\left(\frac{G \cdot x}{H}\right)\right)}{G} \quad (8)$$

$$T_E^{n=2} : \int F(x, H, D)^{n=2} dx \rightarrow \frac{C \cdot D^2 \cdot H \cdot \left( \tan\left(\frac{G \cdot x}{H}\right) - \frac{G \cdot x}{H} \right)}{G} \quad (9)$$

where  $C$  is the stress coefficient of mechanical behavior ( $\text{N} \cdot \text{mm}^{-2}$ ), which is the ratio of the force coefficient of mechanical behavior  $A$  (kN) to that of the square of pressing vessel diameter  $D$  (mm), and  $G$  is the compression coefficient defined as the product of the coefficient of deformation behavior  $B$  ( $\text{mm}^{-1}$ ) and initial pressing height  $H$  (mm) [35]. For the non-linear compression process, the screw press FL 200 pressing chambers or lamella positions (Figure 2) were analyzed theoretically in terms of the initial compression height, deformation, compression ratio and volume of the bulk sample. The screw press geometry parameters for bulk jatropha oilseeds were used for the theoretical analysis of the bulk sample [39].

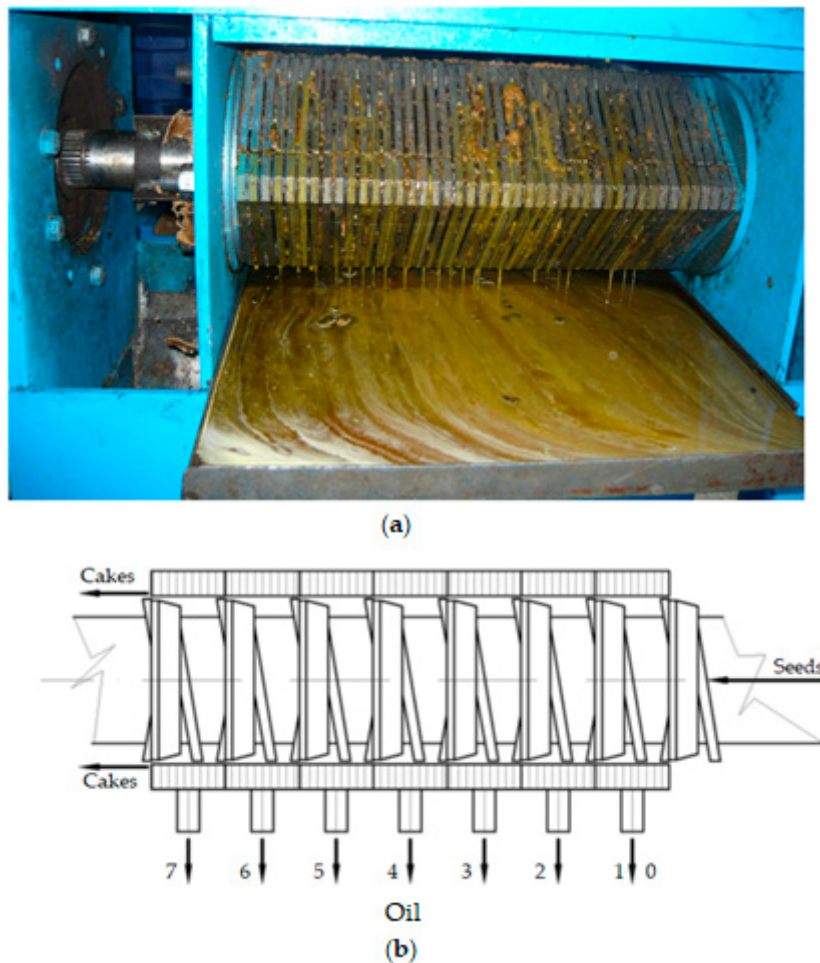


**Figure 2.** (a) Screw press FL 200 with 44 lamellas showing the flow of oil during processing; (b) Screw press geometry with seven pressing sections along the lamellas [38–40].

The theoretical volume of the bulk sample and the screw cross-sectional area were calculated using Equation (10) and Equation (11) as follows:

$$V_V = \frac{\pi}{4} \cdot \left[ D_O^2 - \left( \frac{D_1 + D_2}{2} \right)^2 \right] \cdot (P_T - T_K) \quad (10)$$

$$A_A = \frac{\pi}{4} \cdot \left( D_O^2 - \left( \frac{D_1 + D_2}{2} \right)^2 \right) \quad (11)$$

where  $V_V$  is the theoretical volume of the bulk sample ( $\text{m}^3$ ),  $D_O$  is the screw shaft diameter (mm),  $D_1$  is the screw inner diameter (mm),  $D_2$  is the screw outer diameter (mm),  $P_T$  is the screw pitch diameter (mm) and  $P_k$  is the screw thickness (mm),  $A_A$  is the cross-sectional area of the screw press geometry ( $\text{m}^2$ ). The theoretical pressure and energy at the screw lamella positions (from 0–7) were determined using Equations (8)–(11). Both the experimental and theoretical data were statistically analyzed using MathCAD software, version 15 and STATISITCA, version 13 [41,42].

### 3. Results

The amounts of deformation, oil yield, experimental deformation energy and theoretical deformation energy of the bulk sample in relation to the varying vessel diameters and initial pressing heights are presented in Table 1. From Table 1, it can be seen that the mean total of deformation, oil yield, experimental deformation energy, and theoretical deformation energy at initial pressing heights in relation to the vessel diameters ranged from  $44.61 \pm 1.09$  to  $41.19 \pm 0.42$  mm,  $19.44 \pm 1.01$  to  $13.56 \pm 0.55\%$ ,  $685.59 \pm 6.70$  to  $1263.19 \pm 35.84$  J and  $867.51 \pm 96.19$  to  $1115.61 \pm 92.17$  J respectively. It was observed that the determined or calculated amounts except oil yield increased along with the increase in initial pressing height and vessel diameter. The oil yield, however, decreased with the increase in vessel diameter. The coefficient of variation of the mean values of the above-mentioned parameters in relation to the vessel diameters also ranged from 0.98 to 11.09, 1.51 to 4.41 and 1.02 to 8.26% respectively. Particularly, the percentage difference or error values of the experimental deformation energy against the theoretical deformation energy (Equation (8)) at the various vessel diameters ranged from 5.24 to 23.43%. The lower values of the coefficient of variation greatly show the precision of the obtained results. In addition, the approximately 5% difference or error of the measured and theoretical energy values obtained with vessel diameter 80 mm showed high accuracy of the tangent model (Equation (8)) in comparison with the vessel diameters 60 and 100. The regression coefficients and the whole model with the corresponding statistical evaluation of the compression test data are presented in Tables 2 and 3.

**Table 1.** Compression test data of bulk sample at different vessel diameters and pressing heights.

Vessel Diameter $D$ (mm)	Pressing Height $H$ (mm)	Deformation $x$ (mm)	Oil yield OY (%)	Experimental Deformation Energy $U$	<sup>1</sup> Theoretical Deformation Energy $T_E^{n=1}$ (J)
60	40	$29.66 \pm 0.03$	$18.25 \pm 1.37$	$485.48 \pm 4.43$	$532.28 \pm 3.88$
	60	$45.67 \pm 0.96$	$20.38 \pm 0.88$	$706.45 \pm 6.63$	$820.77 \pm 19.51$
	80	$58.51 \pm 2.27$	$19.69 \pm 0.79$	$864.83 \pm 9.04$	$1249.50 \pm 265.17$
	Mean total	$44.61 \pm 1.09$	$19.44 \pm 1.01$	$685.59 \pm 6.70$	$867.51 \pm 96.19$
	CV (%)	2.44	5.20	0.98	11.09
	PD/PE (%)	-	-	23.43/20.97	
80	40	$27.84 \pm 1.28$	$14.97 \pm 1.41$	$637.52 \pm 23.99$	$676.07 \pm 6.36$
	60	$43.46 \pm 0.44$	$14.82 \pm 0.21$	$904.81 \pm 15.37$	$1004.63 \pm 57.09$
	80	$55.11 \pm 1.14$	$15.07 \pm 0.35$	$1115.38 \pm 0.69$	$1120.00 \pm 48.08$
	Mean total	$42.14 \pm 0.95$	$14.95 \pm 0.66$	$885.90 \pm 13.35$	$933.57 \pm 37.18$
	CV (%)	2.25	4.41	1.51	3.98
	PD/PE (%)	-	-	5.24/5.11	
100	40	$27.33 \pm 0.88$	$13.68 \pm 0.81$	$778.90 \pm 8.24$	$791.83 \pm 40.33$
	60	$40.85 \pm 0.02$	$13.09 \pm 0.05$	$1080.28 \pm 41.21$	$1110.00 \pm 63.64$
	80	$55.38 \pm 0.35$	$13.91 \pm 0.78$	$1446.10 \pm 58.08$	$1445.00 \pm 172.53$
	Mean total	$41.19 \pm 0.42$	$13.56 \pm 0.55$	$1263.19 \pm 35.84$	$1115.61 \pm 92.17$
	CV (%)	1.02	4.06	2.84	8.26
	PD/PE (%)	-	-	12.41/13.23	

CV: Coefficient of Variation, PD: Percentage Difference, PE: Percentage Error, <sup>1</sup> Equation (8).

**Table 2.** Statistical values of the multiple regression analysis of the deformation, oil yield, experimental deformation energy and theoretical deformation energy.

Effect	Deformation $x$ (mm)	Standard Error	$t$ -Value	$P$ -Value
Intercept	7.412	1.718	4.123	<0.05
Vessel diameter $D$ (mm)	-0.086	0.018	-4.826	<0.05
Pressing height $H$ (mm)	0.701	0.018	39.528	<0.05
Effect	Oil Yield $OY$ (%)	Standard Error	$t$ -Value	$P$ -Value
Intercept	26.861	1.718	15.631	<0.05
Vessel diameter $D$ (mm)	-0.147	0.017	-8.672	<0.05
Pressing height $H$ (mm)	0.015	0.017	0.872	>0.05
Effect	Experimental Deformation Energy $U$ (J)	Standard Error	$t$ -Value	$P$ -Value
Intercept	-703.473	86.854	-8.100	<0.05
Vessel diameter $D$ (mm)	10.404	0.857	12.138	<0.05
Pressing height $H$ (mm)	12.703	0.857	14.820	<0.05
Effect	Theoretical Deformation Energy $T_E^{n=1}$ (J)	Standard Error	$t$ -Value	$P$ -Value
Intercept	-431.129	163.676	-2.634	<0.05
Vessel diameter $D$ (mm)	6.202	1.615	3.839	<0.05
Pressing height $H$ (mm)	15.119	1.615	9.359	<0.05

$P$ -Value < 0.05 means statistically significant;  $P$ -Value > 0.05 means statistically non-significant.

**Table 3.** Whole model statistical values of the multiple regression analysis of the parameters determined from the compression test experiment.

Determined Parameters	$R^2$	$F$ -Ratio	$F$ -Critical	$P$ -Value
Deformation $x$ (mm)	0.991	792.876	3.63	<0.05
Oil yield $OY$ (%)	0.835	37.986	3.63	<0.05
Experimental deformation energy $U$ (J)	0.961	183.479	3.63	<0.05
Theoretical deformation energy $T_E^{n=1}$ (J)	0.872	51.174	3.63	<0.05

$P$ -Value < 0.05 or  $F$ -Ratio >  $F$ -Critical means statistically significant.

The ANOVA statistical analysis of the determined tangent curve coefficients of  $A$  and  $B$  from Equation (4) or Equation (7) for a level of significance of 5% using the Mathcad 14 software [40] are given in Tables 4 and 5. At varying initial pressing heights and vessel diameters, the force coefficient  $A$  values applying Equation (5) (Table 4) ranged from  $9.537 \pm 0.151$  to  $8.156 \pm 0.516$ ,  $13.670 \pm 0.170$  to  $10.655 \pm 0.247$  and  $18.170 \pm 0.283$  to  $15.055 \pm 1.011$  kN. The deformation coefficient  $B$  values also ranged from  $0.051 \pm 0.000$  to  $0.027 \pm 0.001$ ,  $0.054 \pm 0.003$  to  $0.028 \pm 0.001$  and  $0.054 \pm 0.001$  to  $0.027 \pm 0.000$  mm<sup>-1</sup>. In comparison to Equation (6) (Table 5), the force coefficient  $A$  values ranged from  $2.931 \pm 0.061$  to  $2.128 \pm 0.284$ ,  $6.434 \pm 0.246$  to  $3.738 \pm 0.168$  and  $12.280 \pm 1.442$  to  $8.431 \pm 1.660$  kN. For the deformation coefficient, similar amounts as indicated above for Equation (5) were observed. From the determined coefficients, it was observed that Equation (5) showed high suitability for fitting the linear compression data compared to Equation (6) with respect to the higher coefficient of determination

values. The experimental and fitted data of the force and deformation curves of the bulk sample for vessel diameter 100 mm in relation to initial pressing heights are illustrated in Figure 1. The fitted data of vessel diameters of 60 and 80 mm showed a similar curve characteristic.

**Table 4.** ANOVA analysis of the tangent model coefficients using Equation (5).

Vessel Diameter <i>D</i> (mm)	Pressing Height <i>H</i> (mm)	<i>A</i> (kN)	<i>B</i> (mm <sup>-1</sup> )	<i>F</i> -Ratio	<i>F</i> -Critical	<i>P</i> -Value	<i>R</i> <sup>2</sup>
60	40	9.537 ± 0.151	0.051 ± 0.000	0.027 ± 0.008	3.867 ± 0.004	0.871 ± 0.018	0.996 ± 0.001
	60	8.624 ± 0.373	0.034 ± 0.001	0.026 ± 0.002	3.861 ± 0.000	0.873 ± 0.005	0.997 ± 0.000
	80	8.156 ± 0.516	0.027 ± 0.001	0.036 ± 0.005	3.860 ± 0.001	0.851 ± 0.011	0.996 ± 0.000
80	40	13.670 ± 0.170	0.054 ± 0.003	0.014 ± 0.004	3.866 ± 0.004	0.906 ± 0.014	0.999 ± 0.000
	60	11.645 ± 0.516	0.035 ± 0.000	0.006 ± 0.001	3.865 ± 0.005	0.939 ± 0.005	0.999 ± 0.000
	80	10.655 ± 0.247	0.028 ± 0.001	0.002 ± 0.000	3.860 ± 0.001	0.968 ± 0.003	1.000 ± 0.001
100	40	18.170 ± 0.283	0.054 ± 0.001	0.012 ± 0.002	3.864 ± 0.001	0.915 ± 0.006	1.000 ± 0.000
	60	15.870 ± 1.117	0.037 ± 0.001	0.003 ± 0.003	3.867 ± 0.001	0.959 ± 0.020	1.000 ± 0.000
	80	15.055 ± 1.011	0.027 ± 0.000	0.0003 ± 0.0005	3.862 ± 0.002	0.988 ± 0.013	1.000 ± 0.000

**Table 5.** ANOVA analysis of the tangent model coefficients using Equation (6).

Vessel Diameter <i>D</i> (mm)	Pressing Height <i>H</i> (mm)	<i>A</i> (kN)	<i>B</i> (mm <sup>-1</sup> )	<i>F</i> -Ratio	<i>F</i> -Critical	<i>P</i> -Value	<i>R</i> <sup>2</sup>
60	40	2.931 ± 0.061	0.049 ± 0.000	0.011 ± 0.004	3.867 ± 0.004	0.918 ± 0.018	0.999 ± 0.000
	60	2.377 ± 0.121	0.032 ± 0.000	0.024 ± 0.003	3.861 ± 0.000	0.876 ± 0.007	0.999 ± 0.000
	80	2.128 ± 0.284	0.026 ± 0.001	0.037 ± 0.013	3.860 ± 0.001	0.848 ± 0.025	0.999 ± 0.001
80	40	6.434 ± 0.246	0.051 ± 0.002	0.058 ± 0.032	3.866 ± 0.004	0.815 ± 0.052	0.998 ± 0.000
	60	4.326 ± 0.160	0.033 ± 0.000	0.062 ± 0.013	3.865 ± 0.005	0.805 ± 0.019	0.998 ± 0.000
	80	3.738 ± 0.168	0.026 ± 0.000	0.107 ± 0.005	3.860 ± 0.001	0.745 ± 0.006	0.997 ± 0.000
100	40	12.280 ± 1.442	0.049 ± 0.001	0.114 ± 0.027	3.864 ± 0.001	0.737 ± 0.030	0.997 ± 0.001
	60	8.934 ± 1.291	0.034 ± 0.001	0.085 ± 0.001	3.867 ± 0.001	0.771 ± 0.001	0.996 ± 0.001
	80	8.431 ± 1.660	0.025 ± 0.000	0.129 ± 0.003	3.862 ± 0.002	0.720 ± 0.004	0.995 ± 0.001

*P*-Value > 0.05 or *F*-Critical > *F*-Ratio means statistically significant. *A* is the force coefficient of mechanical behavior (kN), *B* is the deformation coefficient of mechanical behavior (mm<sup>-1</sup>), *F*-Ratio is the value of the *F*-test, *F*-Critical is the critical value that compares a pair of models, *P*-Value is the significance level used for testing a statistical hypothesis, *R*<sup>2</sup> is the coefficient of determination.

The calculated stress and compression coefficients of the tangent curve model applying Equations (8) and (9) are given in Table 6. For Equation (8), the mean stress coefficient *C* ranged from 2.44 ± 0.10 to 1.64 ± 0.08 N·mm<sup>-2</sup> while the compression coefficient *G* ranged from 2.03 ± 0.03 to 2.17 ± 0.03. In comparison to Equation (9), the mean stress coefficient *C* ranged from 0.69 ± 0.04 to 0.99 ± 0.14 N·mm<sup>-2</sup> while the compression coefficient *G* ranged from 1.97 ± 0.02 to 2.03 ± 0.03. Using both Equations (8) and (9), the stress coefficients decreased along with the increase in initial pressing heights and vessel diameters. However, the mean total of the stress coefficients (Equation (8)) in relation to the initial pressing heights decreased along with the increase in vessel diameter while for Equation (9), the stress coefficients increased. On the other hand, the compression coefficients did not show either a positive or negative linear dependency in relation to the initial pressing heights and vessel diameters. But, the mean total of the compression coefficients increased linearly with regards to the vessel diameters while that of Equation (9), both increasing and decreasing amounts were observed. Therefore, it can be said that the bulk sample initial pressing heights and vessel diameters have an effect on the stress and compression coefficients of the tangent curve model. The coefficient of variation of the mean values of the stress and compression coefficients using Equations (8) and (9) in relation to the vessel diameters also ranged from 1.02 to 5.79, 1.48 to 3.95 and 1.38 to 14.14%, respectively.

**Table 6.** Stress and compression coefficients of the tangent curve model at different vessel diameters and pressing heights.

Vessel Diameter $D$ (mm)	Pressing Height $H$ (mm)	<sup>1</sup> Stress Coefficient $C$ (N·mm <sup>-2</sup> )	<sup>1</sup> Compression Coefficient $G$	<sup>2</sup> Stress Coefficient $C$ (N·mm <sup>-2</sup> )	<sup>2</sup> Compression Coefficient $G$
60	40	2.65 ± 0.04	2.04 ± 0.00	0.82 ± 0.02	1.96 ± 0.00
	60	2.41 ± 0.11	2.01 ± 0.04	0.66 ± 0.03	1.92 ± 0.00
	80	2.27 ± 0.15	2.12 ± 0.06	0.60 ± 0.08	2.04 ± 0.06
	Mean total	2.44 ± 0.10	2.03 ± 0.03	0.69 ± 0.04	1.97 ± 0.02
	CV (%)	4.10	1.48	5.79	1.02
80	40	2.14 ± 0.02	2.16 ± 0.11	1.01 ± 0.04	2.02 ± 0.08
	60	1.82 ± 0.08	2.10 ± 0.00	0.68 ± 0.02	1.98 ± 0.00
	80	1.67 ± 0.04	2.20 ± 0.06	0.59 ± 0.02	2.08 ± 0.00
	Mean total	1.88 ± 0.05	2.15 ± 0.06	0.76 ± 0.03	2.03 ± 0.03
	CV (%)	2.66	2.79	3.95	1.48
100	40	1.82 ± 0.03	2.16 ± 0.06	1.23 ± 0.14	1.94 ± 0.03
	60	1.59 ± 0.11	2.19 ± 0.04	0.89 ± 0.13	2.01 ± 0.04
	80	1.51 ± 0.11	2.16 ± 0.00	0.85 ± 0.16	1.96 ± 0.06
	Mean total	1.64 ± 0.08	2.17 ± 0.03	0.99 ± 0.14	1.97 ± 0.04
	CV (%)	4.88	1.38	14.14	2.03

CV: Coefficient of variation, <sup>1</sup> Equation (8), <sup>2</sup> Equation (9).

The mean total values of the stress and compression coefficients obtained from Equations (8) and (9) in relation to the initial pressing heights and vessel diameters were further used to determine the amounts of screw force, pressure and energy along the screw press FL 200 pressing chambers. The data on the theoretical screw pressure and energy is indicated in Tables 7 and 8. The complete data on the screw force is not presented here since the pressure was calculated as the ratio of the screw force to the screw cross-sectional area [31,39]. Using Equation (8), in relation to the vessel diameters and screw lamella positions, the screw pressure amounts ranged from 1.438 to 48.412 MPa, 1.808 to 39.466 MPa and 2.179 to 33.816 MPa. The screw energy values ranged from 90.699 to 166.074 J, 102.158 to 161.088 J and 112.451 to 155.926 J. Comparing the results mentioned above to Equation (9), the amounts of the screw pressure ranged from 0.31 to 74.95 MPa, 0.51 to 58.13 MPa and 0.788 to 45.994 MPa. The screw energy values ranged from 12.616 to 119.201 J, 19.247 to 122.65 J and 28.182 to 125.578 J. It was observed that the screw pressure values increased along with the screw lamella positions. Increasing the vessel diameter also increased the pressure and energy values. Higher values were obtained for Equation (8) in comparison to Equation (9) for all vessel diameters. In addition, for both Equations (8) and (9), the cumulative amounts of pressure decreased with increasing vessel diameters while energy increased. The regression coefficients and the whole model with the corresponding statistical evaluation of the theoretical pressure and energy are presented in Tables 9 and 10.

**Table 7.** Theoretical pressure at the screw press lamella positions.

Screw Lamella Positions $S_L$	Vessel Diameter 60 mm		Vessel Diameter 80 mm		Vessel Diameter 100 mm	
	Screw Pressure $S_{PD60}$ (MPa)	Cumulative $S_{PD60}$ (MPa)	Screw Pressure $S_{PD80}$ (MPa)	Cumulative $S_{PD80}$ (MPa)	Screw Pressure $S_{PD100}$ (MPa)	Cumulative $S_{PD100}$ (MPa)
0	0	0	0	0	0	0
1	1.438 <sup>1</sup>	1.438	1.808	1.808	2.179	2.179
	0.31 <sup>2</sup>	0.31	0.51	0.51	0.788	0.788
2	6.189 <sup>1</sup>	7.627	7.093	8.901	7.745	9.924
	3.533 <sup>2</sup>	3.843	4.899	5.409	6.156	6.944
3	7.068 <sup>1</sup>	14.695	7.999	16.9	8.631	18.555
	4.325 <sup>2</sup>	8.168	5.849	11.258	7.189	14.133

Table 7. Cont.

Screw Lamella Positions $S_L$	Vessel Diameter 60 mm		Vessel Diameter 80 mm		Vessel Diameter 100 mm	
	Screw Pressure $S_{PD60}$ (MPa)	Cumulative $S_{PD60}$ (MPa)	Screw Pressure $S_{PD80}$ (MPa)	Cumulative $S_{PD80}$ (MPa)	Screw Pressure $S_{PD100}$ (MPa)	Cumulative $S_{PD100}$ (MPa)
4	9.483 <sup>1</sup>	24.178	10.4	27.3	10.907	29.462
	6.749 <sup>2</sup>	14.917	8.62	19.878	10.009	24.142
5	11.183 <sup>1</sup>	35.361	12.022	39.322	12.392	41.854
	8.653 <sup>2</sup>	23.57	10.66	30.538	11.962	36.104
6	18.137 <sup>1</sup>	53.498	18.177	57.499	17.729	59.583
	17.816 <sup>2</sup>	41.386	19.41	49.948	19.555	55.659
7	48.412 <sup>1</sup>	101.91	39.466	96.965	33.816	93.399
	74.95 <sup>2</sup>	116.336	58.13	108.078	45.994	101.653

<sup>1</sup> Equation (8), <sup>2</sup> Equation (9).

Table 8. Screw energy at the screw press lamella positions.

Screw Lamella Positions $S_L$	Vessel Diameter 60 mm		Vessel Diameter 80 mm		Vessel Diameter 100 mm	
	Screw Energy $S_{ED60}$ (J)	Cumulative $S_{ED60}$ (J)	Screw Energy $S_{ED80}$ (J)	Cumulative $S_{ED80}$ (J)	Screw Energy $S_{ED100}$ (J)	Cumulative $S_{ED100}$ (J)
0	0	0	0	0	0	0
1	90.699 <sup>1</sup>	90.699	102.158	102.158	112.451	112.451
	12.616 <sup>2</sup>	12.616	19.247	19.247	28.182	28.182
2	170.249 <sup>1</sup>	260.948	184.622	286.78	194.879	307.33
	55.066 <sup>2</sup>	67.682	76.361	95.608	99.792	127.974
3	172.597 <sup>1</sup>	433.545	186.288	473.068	195.718	503.048
	59.053 <sup>2</sup>	126.735	80.894	176.502	104.353	232.327
4	175.816 <sup>1</sup>	609.361	187.595	660.663	194.942	697.99
	67.895 <sup>2</sup>	194.63	90.249	266.751	112.925	345.252
5	176.689 <sup>1</sup>	786.05	187.189	847.852	193.258	891.248
	72.915 <sup>2</sup>	267.545	95.114	361.865	116.868	462.12
6	175.856 <sup>1</sup>	961.906	181.912	1029.764	184.054	1075.302
	87.64 <sup>2</sup>	355.185	107.267	469.132	124.518	586.638
7	166.074 <sup>1</sup>	1127.98	161.088	1190.852	155.926	1231.228
	119.201 <sup>2</sup>	474.386	122.65	591.782	125.578	712.216

<sup>1</sup> Equation (8), <sup>2</sup> Equation (9).

Table 9. Statistical values of the multiple regression analysis of the pressure and energy at the screw lamella positions.

Effect	Screw Pressure $S_P$ (MPa)	Standard Error	$t$ -Value	$P$ -Value
Intercept	-5.311	8.904	-0.596	>0.05
Screw lamella positions $S_L$	5.423	0.645	8.412	<0.05
Vessel diameter $D$ (mm)	-0.036	0.090	-0.401	>0.05
Model fitting value $n$ (-)	1.408	2.954	0.477	>0.05
Effect	Screw Energy $S_E$ (J)	Standard Error	$t$ -Value	$P$ -Value
Intercept	119.057	31.643	3.763	<0.05
Screw lamella positions $S_{LP}$ (-)	17.156	2.291	7.488	<0.05
Vessel diameter $D$ (mm)	0.533	0.321	1.658	>0.05
Model fitting value $n$ (-)	-73.819	10.499	-7.031	<0.05

 $P$ -Value < 0.05 means statistically significant;  $P$ -Value > 0.05 means statistically non-significant.

**Table 10.** Whole model statistical values of the multiple regression analysis of the calculated parameters at the screw press lamella positions.

Calculated Parameters	$R^2$	F-Ratio	F-Critical	P-Value
Screw pressure $S_P$ (MPa)	0.618	23.714	2.419	<0.05
Screw energy $S_E$ (J)	0.711	36.086	2.419	<0.05

$P$ -Value < 0.05 or  $F$ -Ratio >  $F$ -Critical means statistically significant.

#### 4. Discussion

The parameters determined from the linear compression test were deformation, oil yield, experimental deformation energy and theoretical deformation energy. Based on the whole model of the multiple regression analysis, the vessel diameter and bulk sample initial pressing height had a significant effect ( $P$ -Value < 0.05) or ( $F$ -Ratio >  $F$ -Critical) (Table 3) on the above mentioned determined parameters. The independent variables (vessel diameter and pressing height) would contribute significantly ( $P$ -Value < 0.05) to the prediction of the dependent variables (deformation, experimental deformation energy and theoretical deformation energy). However, for oil yield, the initial pressing height would not contribute significantly ( $P$ -Value > 0.05). This means that the coefficient of the initial pressing height will not be used in the regression model to predict the oil yield of sunflower bulk oilseeds. The force coefficient of mechanical behavior  $A$  (kN) and deformation coefficient of mechanical behavior  $B$  ( $\text{mm}^{-1}$ ) of the tangent curve model were statistically significant ( $P$ -Value > 0.05) or ( $F$ -Critical >  $F$ -Ratio) according to the ANOVA analysis using MathCAD, version 15 [41]. The determined coefficients can be used to describe the force-deformation curves of sunflower bulk oilseeds at a maximum force of 200 kN and speed of  $5 \text{ mm min}^{-1}$ . Theoretically, the area under the force-deformation curves is the deformation energy [32,34]. The tangent curve model with the corresponding fitting value of  $n = 1$  (Equation (8)) showed higher suitability for describing the linear compression curves compared to the fitting value of  $n = 2$  (Equation (9)) based on the coefficient of determination ( $R^2$ ) values.

From the multiple regression results of the non-linear compression process, the screw lamella position showed statistically significant ( $P$ -Value < 0.05) (Table 9) for predicting the screw pressure. However, the vessel diameter and tangent model fitting value were not statistically significant ( $P$ -Value > 0.05). On the other hand, the screw lamella position and model fitting value were statistically significant ( $P$ -Value < 0.05) (Table 9) for predicting the screw energy in comparison to the vessel diameter which was not statistically significant ( $P$ -Value > 0.05). Based on the whole model statistical values (Table 10), the vessel diameter, screw lamella position and tangent model fitting value had significant influence ( $P$ -Value < 0.05) or ( $F$ -Ratio >  $F$ -Critical) on the theoretical amounts of screw pressure and energy respectively. Comparing the results of the current study (using Equation (8)) to the previously published study [39,40], it was found that the bulk oil palm kernels had higher amounts of the theoretical pressure along the screw lamella positions from (0–6) for all vessel diameters followed by sunflower bulk oilseeds and then jatropha bulk oilseeds. However, at pressing chamber positions 6 and 7, higher amounts of pressure were obtained for sunflower bulk oilseeds followed by bulk oil palm kernels and then jatropha bulk oilseeds. This trend was similar to the amounts of the theoretical energy with the exception of vessel diameter of 100 mm, where sunflower bulk oilseeds produced higher amounts of the theoretical energy along the screw lamellas. Actually, the experimental processing parameters (maximum force of 200 kN and speed of  $5 \text{ mm} \cdot \text{min}^{-1}$ ) for sunflower bulk oilseeds and oil palm bulk kernels were similar compared to jatropha bulk oilseeds where the maximum force and speed were 100 kN and  $1 \text{ mm} \cdot \text{s}^{-1}$  [39]. In the previous study [39], Equation (9) was only examined for the jatropha bulk oilseeds. However, for sunflower bulk oilseeds (present study) and oil palm bulk kernels (previous study) [39], both Equations (8) and (9) were investigated, and similar trend of the results was obtained as already described above. Based on these comparisons, it can be concluded that

more energy would be required for recovering the oil from oil palm bulk kernels than sunflower bulk oilseeds when using the screw press FL 200. This conclusion, however, cannot be stated for jatropha bulk oilseeds for now until similar processing parameters are studied. Furthermore, based on the multiple linear regression results, the screw lamella position and fitting curve value of the tangent model (Equations (8) and (9)) were found to significantly ( $P$ -Value  $< 0.05$ ) influence the amount of the theoretical energy of both sunflower bulk oilseeds and oil palm bulk kernels while the vessel diameter had no significant effect ( $P$ -Value  $> 0.05$ ). The screw lamella position also had a significant effect on the theoretical amounts of force and pressure while the vessel diameter and fitting curve value of the tangent model did not show significant influence. Most importantly, the strain or compression ratio which is the ratio of deformation to the initial pressing height is influenced by the pressing factors including moisture content and friction [35]. Therefore, the compression ratio variable in Equation (8) and Equation (9) was divided by the coefficient of the pressing factors which was estimated for each vessel diameter (60, 80 and 100 mm) in relation to the processing parameters. For jatropha bulk oilseeds at a maximum force of 100 kN [38], the estimated pressing factors coefficients values of 1.42, 1.55 and 1.74 in increasing order of the vessel diameter were reported. In the case of sunflower bulk oilseeds at a maximum force of 200 kN, the coefficient values of 1.226, 1.384 and 1.537 were observed for Equation (8) and 1.208, 1.328 and 1.436 for Equation (9). For oil palm bulk kernels, the values of the pressing coefficients were 1.637, 2.14 and 2.89 for Equation (8) and 1.59, 1.88 and 2.42 for Equation (9). The tangent curve models (Equations (8) and (9)) suggest that the coefficients of the pressing factors should be determined experimentally to obtain adequate knowledge on the optimum processing parameters of the screw press FL 200.

In the literature, it is obvious that many models have been applied extensively on the modeling of oilseeds or food processing engineering aimed at understanding the aerodynamics and biophysical or physical properties as well as optimizing the processing parameters. Some of these models include response surface methodology, artificial neural network, adaptive neuro-fuzzy inference system, fuzzy logic design [43–49]. However, the tangent curve mathematical model applied in this present study and previously published studies show reliability for describing the linear and non-linear compression processes of bulk oilseeds based on the experimental or model boundary conditions [35–37]. Future studies would consider examining the above-mentioned models in the linear and non-linear compression processes of selected bulk oilseeds.

## 5. Conclusions

Based on the results presented and discussed, it was revealed that the coefficients of the independent variables (vessel diameter and initial pressing height) in the determined regression model would contribute significantly to the prediction of the dependent variables (deformation, experimental deformation energy and theoretical deformation energy of sunflower bulk oilseeds in the linear compression process. The initial pressing height coefficient in the regression model had no significant effect on the oil yield in comparison to the vessel diameter which had a significant effect. The tangent curve model with the corresponding fitting value of  $n = 1$  (Equation (8)) showed high suitability for describing theoretically the experimental force-deformation curves as well as the deformation energy of sunflower bulk oilseeds. Using (Equation (8)), the screw pressure amounts along the screw press FL 200 pressing chamber positions (1–7) ranged from 1.438 to 48.412 MPa, 1.808 to 39.466 MPa and 2.179 to 33.816 MPa for vessel diameters 60, 80 and 100 mm while the screw energy values ranged from 90.699 to 166.074 J, 102.158 to 161.088 J and 112.451 to 155.926 J. The coefficients of the screw lamella position and tangent curve model fitting value in the determined regression model showed statistical significance for predicting the theoretical screw energy. The cumulative amounts of the theoretical screw pressure along the screw press FL 200 pressing chamber positions (1–7) decreased with increasing vessel diameters while the screw energy increased. The lower values of the coefficient of variation and percentage difference or error of the measured and theoretical data obtained in the linear compression process proved high precision and accuracy for determining the non-linear compression parameters

(screw energy and pressure). The modeling processes described in this study would be applied on other commonly used bulk oilseeds such as soybean, sesame, rapeseeds to fully understand their mechanical behaviors in both the linear and non-linear pressing conditions and also to determine the optimal processing parameters of the mechanical screw FL 200 using response surface methodology.

**Author Contributions:** Conceptualization, D.H., and A.K.; Funding acquisition, D.H.; Methodology, D.H., A.K., and R.S.; Writing—original draft, A.K. and D.H.; Writing—review and editing, A.K., D.H., H.A., and R.S.

**Funding:** This research through the project “supporting the development of international mobility of research staff at CULS Prague, grant number CZ.02.2.69/0.0/0.0/16\_027/0008366” was funded by “EU, Managing Authority of the Czech Operational Programme Research, Development and Education”, and “The APC was funded by the project “supporting the development of international mobility of research staff at CULS Prague, grant number CZ.02.2.69/0.0/0.0/16\_027/0008366”.

**Acknowledgments:** The Authors would like to thank the funding providers for the financial support.

**Conflicts of Interest:** The authors declare no conflict of interest.

## References

- Macedo, T.d.O.; Pereira, R.G.; Pardal, J.M.; Soares, A.S.; Lameira, V.d.J. Viscosity of vegetable oils and biodiesel and energy generation. *J. Chem. Mol. Eng.* **2013**, *7*, 251–256.
- Chapius, A.; Blin, J.; Carre, P.; Lecomte, D. Separation efficiency and energy consumption of oil expression using a screw-press: The case of *Jatropha curcas* L. seeds. *Ind. Crop Prod.* **2014**, *52*, 752–761. [[CrossRef](#)]
- Tamas, K.; Foldesi, B.; Radics, J.P.; Jori, I.J.; Fenyvesi, L. A simulation model for determining the mechanical properties of rapeseed using the discrete element method. *Period. Polytech.-Civ. Eng.* **2015**, *59*, 575–582. [[CrossRef](#)]
- Lazaroiu, G.; Traista, E.; Badulescu, C.; Orban, M.; Plesea, V. Sustainable combined utilization of renewable forest resources and coal in Romania. *Environ. Eng. Manag. J.* **2008**, *7*, 227–232. [[CrossRef](#)]
- Bansal, N.; Dhaliwal, A.S.; Mann, K.S. Dielectric characterization of rapeseed (*Brassica napus* L. from 10 to 3000 MHz. *Biosyst. Eng.* **2016**, *143*, 1–8. [[CrossRef](#)]
- Zafar, S.; Li, Y.-L.; Li, N.-N.; Zhu, K.-M.; Tan, X.-L. Recent advances in enhancement of oil content in oilseed crops. *J. Biotechnol.* **2019**, *301*, 35–44. [[CrossRef](#)] [[PubMed](#)]
- Mpagalile, J.J.; Hanna, M.A.; Weber, R. Seed oil extraction using a solar powered screw press. *Ind. Crop Prod.* **2007**, *25*, 101–107. [[CrossRef](#)]
- Mpagalile, J.J.; Hanna, M.A.; Weber, R. Design and testing of a solar photovoltaic operated multi-seeds oil press. *Renew. Energy* **2006**, *31*, 1855–1866. [[CrossRef](#)]
- Venter, M.J.; Willems, P.; Kuipers, N.J.M.; De Haan, A.B. Gas assisted mechanical expression of cocoa butter from cocoa nibs and edible oils from oilseeds. *J. Supercrit. Fluids* **2006**, *37*, 350–358. [[CrossRef](#)]
- Venter, M.J.; Kuipers, N.J.M.; de Haan, A.B. Modelling and experimental evaluation of high-pressure expression of cocoa nibs. *J. Food Eng.* **2007**, *80*, 1157–1170. [[CrossRef](#)]
- Willems, P.; Kuipers, N.J.M.; De Haan, A.B. Hydraulic pressing of oilseeds: Experimental determination and modeling of yield and pressing rates. *J. Food Eng.* **2008**, *89*, 8–16. [[CrossRef](#)]
- Khan, L.M.; Hanna, M.A. Expression of oil from oilseeds—A review. *J. Agric. Eng. Res.* **1983**, *28*, 495–503. [[CrossRef](#)]
- Bargale, P.C. Mechanical Oil Expression from Selected Oilseeds under Uniaxial Compression. Ph.D. Thesis, University of Saskatchewan, Saskatoon, SK, Canada, 1997; p. 310.
- Singh, J.; Bargale, P.C. Development of a small capacity double stage compression screw press for oil expression. *J. Food Eng.* **2000**, *43*, 75–82. [[CrossRef](#)]
- Achten, W.M.J.; Mathijs, E.; Verchot, L.; Singh, V.P.; Aerts, R.; Muys, B. *Jatropha* biodiesel fueling sustainability? Biofuels Bioprod. *Biorefining* **2007**, *1*, 283–291. [[CrossRef](#)]
- Ogunsina, B.S.; Owolarafe, O.K.; Olatunde, G.A. Oil point pressure of cashew (*Anacardium occidentale*) kernels. *Int. Agrophys.* **2008**, *22*, 53–59. [[CrossRef](#)]
- Pradhan, R.C.; Mishra, S.; Naik, S.N.; Bhatnagar, N.; Vijay, V.K. Oil expression from *Jatropha* seeds using a screw press expeller. *Biosyst. Eng.* **2011**, *109*, 158–166. [[CrossRef](#)]
- Singh, K.K.; Wiesenborn, D.P.; Tostenson, K.; Kangas, N. Influence of moisture content and cooking on screw pressing of crambe seed. *J. Am. Oil Chem. Soc.* **2002**, *79*, 165–170. [[CrossRef](#)]

19. Adeeko, K.A.; Ajibola, O.O. Processing factors affecting yield and quality of mechanically expressed groundnut oil. *J. Agric. Eng. Res.* **1990**, *45*, 31–43. [[CrossRef](#)]
20. Deli, S.; Farah Masturah, M.; Tajul Aris, Y.; Wan Nadiyah, W.A. The effects of physical parameters of the screw press oil expeller on oil yield from *Nigella sativa* L. seeds. *Int. Food Res. J.* **2011**, *18*, 1367–1373.
21. Karaj, S.; Muller, J. Optimizing mechanical oil extraction of *Jatropha curcas* L. seeds with respect to press capacity, oil recovery and energy efficiency. *Ind. Crop Prod.* **2011**, *34*, 1010–1016. [[CrossRef](#)]
22. Savoie, R. Screw pressing application to oilseeds. *Ref. Modul. Food Sci.* **2017**, 1–3. [[CrossRef](#)]
23. Sorin-Stefan, B.; Ionescu, M.; Voicu, G.; Ungureanu, N.; Vladut, V. Calculus Elements for Mechanical Presses in Oil Industry. *Food Ind.* **2013**, *21*, 471–479. [[CrossRef](#)]
24. Terzaghi, K. *Theoretische Bodenmechanik*; Springer: Berlin, Germany, 1954.
25. Fasina, O.O.; Ajibola, O.O. Development of equations for the yield of oil expressed from conophor nut. *J. Agric. Eng. Res.* **1990**, *46*, 45–53. [[CrossRef](#)]
26. Lanoisellé, J.-L.; Vorobyov, I.; Bouvier, J.-M.; Piar, G. Modeling of solid-liquid expression for cellular materials. *AIChE J.* **1996**, *42*, 2057–2068. [[CrossRef](#)]
27. Mrema, G.C.; McNulty, P.B. Mathematical model of mechanical oil expression from oilseeds. *J. Agric. Eng. Res.* **1985**, *31*, 361–370. [[CrossRef](#)]
28. Shirato, M.; Murase, T.; Iwata, M.; Nakatsuka, S. The Terzaghi-Voight combined model for constant-pressure consolidation of filter cakes and homogeneous semi-solid materials. *Chem. Eng. Sci.* **1986**, *41*, 3213–3218. [[CrossRef](#)]
29. Bogaert, L.; Mathieu, H.; Mhemdi, H.; Vorobiev, E. Characterization of oilseeds mechanical expression in an instrumental pilot screw press. *Ind. Crop Prod.* **2018**, *121*, 106–113. [[CrossRef](#)]
30. ISI. *Indian Standard Methods for Analysis of Oilseeds*; IS:3579; Indian Standard Institute: New Delhi, India, 1996.
31. Blahovec, J. *Agromaterials Study Guide*; Czech University of Life Sciences Prague: Prague, Czech Republic, 2008; p. 7.
32. Demirel, C.; Kabutey, A.; Herak, D.; Gurdil, G.A.K. Numerical estimation of deformation energy of selected bulk oilseeds in compression loading. *IOP Conf. Ser. Mater. Sci. Eng.* **2017**, *237*, 1–5. [[CrossRef](#)]
33. Kabutey, A.; Herak, D.; Mizera, C.; Hrabě, P. Mathematical description of loading curves and deformation energy of bulk oil palm kernels. *Agron. Res.* **2018**, *16*, 1686–1697. [[CrossRef](#)]
34. Ivanova, T.; Kabutey, A.; Herak, D.; Demirel, C. Estimation of energy requirement of *Jatropha curcas* L. seedcake briquettes under compression loading. *Energies* **2018**, *11*, 1980. [[CrossRef](#)]
35. Herák, D.; Kabutey, A.; Divišová, M.; Simanjuntak, S. Mathematical model of mechanical behaviour of *Jatropha curcas* L. seeds under compression loading. *Biosyst. Eng.* **2013**, *114*, 279–288. [[CrossRef](#)]
36. Sigalingging, R.; Herák, D.; Kabutey, A.; Čestmír, M.; Divišová, M. Tangent curve function description of mechanical behaviour of bulk oilseeds: A review. *Sci. Agric. Bohem.* **2014**, *45*, 259–264. [[CrossRef](#)]
37. Sigalingging, R.; Herák, D.; Kabutey, A.; Dajbych, O.; Hrabě, P.; Mizera, C. Application of a tangent curve mathematical model for analysis of the mechanical behaviour of sunflower bulk seeds. *Int. Agrophys.* **2015**, *29*, 517–524. [[CrossRef](#)]
38. Kabutey, A.; Herak, D.; Hanus, J. Screw press performance for oil extraction from *Jatropha curcas* L. seeds of different moisture content. *Sci. Agric. Bohem.* **2010**, *41*, 225–230.
39. Kabutey, A.; Herak, D.; Hanus, J.; Choteborsky, R.; Dajbych, O.; Sigalingging, R.; Akangbe, O.L. Prediction of pressure and energy requirement of *Jatropha curcas* L. bulk seeds under non-linear pressing. In Proceedings of the 6th International Conference TAE, Prague, Czech Republic, 7–9 September 2016; pp. 262–269.
40. Kabutey, A.; Herak, D.; Mizera, C.; Hrabě, P. Theoretical analysis of force, pressure and energy distributions of bulk palm kernels along the screwline of a mechanical screw press FL 200. *Agron. Res.* **2019**, *17*. [[CrossRef](#)]
41. *Mathsoft*; Parametric Technology Corporation: Needham, MA, USA, 2014.
42. *Statsoft*; StatSoft, Inc.: Tulsa, OK, USA, 2013.
43. Mohammad, G.; Seid, M.J.; Farzanehm, V.; Narges, M. Kinetics modelling of colour deterioration during thermal processing of tomato paste with the use of response surface methodology. *Heat Mass Transf.* **2018**, *54*, 3663–3671. [[CrossRef](#)]
44. Farzaneh, V.; Ghodsvali, A.; Bakhshabadi, H.; Dolatabadi, Z.; Farzaneh, F.; Carvalho, I.S.; Sarabandi, K. Screening of the alterations in qualitative characteristics of grape under the impacts of storage and harvest times using artificial neural network. *Evol. Syst.* **2018**, *9*, 81–89. [[CrossRef](#)]

45. Jalili, F.; Jafari, S.M.; Emam-Djomeh, Z.; Malekjani, N. Optimization of Ultrasound-Assisted Extraction of Oil from Canola Seeds with the Use of Response Surface Methodology. *Food Anal. Methods* **2018**, *11*, 598–612. [[CrossRef](#)]
46. Farzaneh, V.; Bakhshabadi, H.; Gharekhani, M.; Mohammad, G.; Farzaneh, F.; Rashidzadeh, S.; Carvalho, I.S. Application of an adaptive neuro\_fuzzy inference system (ANFIS) in the modeling of rapeseeds' oil extraction. *Food Process Eng.* **2017**, *40*, e12562. [[CrossRef](#)]
47. Ghodsvali, A.; Farzaneh, V.; Bakhshabadi, H.; Zare, Z.; Karami, Z.; Mokhtarian, M.; Carvalho, I.S. Screening of the aerodynamic and biophysical properties of barley malt. *Int. Agrophys.* **2016**, *30*, 457–464. [[CrossRef](#)]
48. Farzaneh, V.; Ghodsvali, A.; Bakhshabadi, H.; Mohammad, G.; Dolatabadi, Z.; Carvalho, I.S. Modelling of the selected physical properties of the fava bean with various moisture contents using fuzzy logic design. *Food Process Eng.* **2016**, *40*, e12366. [[CrossRef](#)]
49. Jabrayili, S.; Farzaneh, V.; Zare, Z.; Bakhshabadi, H.; Babazadeh, Z.; Mokhtarian, M.; Carvalho, I.S. Modelling of mass transfer kinetic in osmotic dehydration of kiwifruit. *Int. Agrophys.* **2016**, *30*, 185–191. [[CrossRef](#)]



© 2019 by the authors. Licensee MDPI, Basel, Switzerland. This article is an open access article distributed under the terms and conditions of the Creative Commons Attribution (CC BY) license (<http://creativecommons.org/licenses/by/4.0/>).